Research Paper　　　　　　　　　　　　　　　　　　　　　Open Access

Spectroscopic Properties of Pr^{3+} Ions Embedded in Different Multi Component Phosphate Glasses

B Haritha, V Reddy Prasad, S Damodaraiah, Y C Ratnakaram*

Department of Physics, Sri Venkateswara University, Tirupati-517502
Corresponding Author:Y.C. Ratnakaram

ABSTRACT: *Pr^{3+} doped multi component phosphate glasses were prepared by conventional melt quenching technique. The structures were characterized by XRD, Fourier transform infrared and solid-state ^{31}P NMR techniques. Optical absorption and emission spectra of Pr^{3+} doped Li, Ba, Mg and Ca phosphate glasses have been studied. Optical properties of rare earth ion were characterized through optical absorption and emission spectra using Judd-Ofelt theory. Judd-Ofelt intensity parameters Ω_λ (λ=2, 4 ,6) are calculated from the absorption spectra, which inturn used to derive the radiative properties such as radiative transition probabilities(A_R), radiative lifetimes(τ_R) and branching ratios(β). An attempt has been made to discuss structural changes considering the hypersensitive transitions and covalency of rare earth oxygen (RE-O) bonds for the present glass systems. From the emission spectra, peak emission cross- sections (σ_p) are obtained for the observed emission bands of Pr^{3+} ion in all these phosphate glasses. Variation of emission cross-sections with the glass matrix has been studied. Further, decay time constants are estimated from the decay profiles of Pr^{3+}-doped different multi component glasses.*

Keywords: *phosphate glass; solid-state ^{31}P NMR; Absorption; Emission; radiative lifetimes; branching ratio; stimulated emission cross-section; decay time.*

I. INTRODUCTION

Different host materials doped with Rare Earth (RE) ions find potential industrial applications in solid state lasers, upconverters, optical amplifiers, phosphors and sensors. The knowledge on the optical properties of RE ions in glasses is very important in order to optimize the best ion host combination [1-4]. Glasses accept RE ions without inducing crystallization and exhibit large optical transparency window covering ultraviolet (UV), visible (VIS) and near infrared (NIR) regions [5-7]. RE doped glasses have been used in optical devices such as solid state lasers, color displays, imaging and optical telecommunication industries because of their high efficient luminescence in the visible and infrared regions due to 4f-4f intra configuration transitions of rare earth ions. The optical properties of rare earth ions in glasses depend on the chemical compositions of the glass matrix which determine the structure and nature of the bonds [8-10].

Phosphate glasses are potentially important host materials for developing RE doped optical devices. Phosphate glasses have excellent transparency and good mechanical and thermal stability. They act as good hosts for large concentrations of doping RE ions with good homogeneity. Phosphate glasses generally offer higher solubility of RE dopants, thus the amount of active ions can be significantly increased. Phosphate glasses with low melting temperatures, high thermal expansion coefficient and other optical properties make these glasses as potential candidates for many applications such as sealing materials, medical use, solid state electrolytes and high energy lasers [11-14].

Recently Deopa et al. studied spectroscopic studies of Pr^{3+} doped LiPbAlB glasses for visible reddish orange luminescent device applications [15]. Han et al. observed Pr^{3+} doped phosphate glasses for fiber amplifiers operating at 1.38-1.53 μm of the fifth optical telecommunication window [16]. Herrera et al. reported multichannel emission from Pr^{3+} doped heavy-metal oxide glass (B_2O_3-PbO-GeO$_2$-Bi$_2$O$_3$) for broad band signal amplification [17]. Koepke et al. have studied the spectroscopic properties of lead-gallium oxyfluoride glasses and glass-ceramics activated by Pr^{3+} ions. Kaewjaeng et al. reported optical and luminescence properties of Pr^{3+} in Gd$_2$O$_3$-CaO-SiO$_2$-B$_2$O$_3$ glasses [18].

The present work mainly focuses on optimization of Pr^{3+} doped host glass composition which exhibit better optical, radiative and luminescence properties. Structural modifications imposed by the variation of multicomponent doped glasses were studied by XRD, SEM, Fourier transform infrared (FTIR) and solid-state NMR. Foes was laid on to report optical absorption and luminescence properties of multicomponent Pr^{3+} doped different phosphate glasses. An attempt is also made to study the radiative properties like radiative transition probabilities (A_R), radiative lifetimes (τ_R), branching ratios (β_R), absorption cross sections (Σ), and peak emission cross sections (σ_p) using Judd-Ofelt (J-O) theory.

II. EXPERIMENTAL

The glass samples used in the present work were prepared by conventional melt quenching technique with the following chemical compositions $(69-x)P_2O_5+15Na_2CO_3+MCO_3+xPr_6O_{11}$ (where, x=1.0 mol% and M=Li, Mg, Ca, Ba) and appropriate amounts of the chemicals are made into fine powder in an agate mortar and thoroughly ground. The homogenously mixed chemicals were then heated in an electric furnace at about 1100^0C for 1 hour in porcelain crucible to obtain glass melt. The melt was quenched between two well polished brass plates. The density of glass samples was measured using Archimedes' principle with water as an immersion liquid. The refractive indices were measured using an Abbe refractometer. The absorption spectra were recorded at room temperature using JASCO V–570 spectrophotometer. The fluorescence spectra were recorded with FLS 920, Edinburg using xenon lamp as excitation source. XRD profiles of these glasses were recorded in the range of $10-70^0$ with RIGAKU X-ray diffractometer. The SEM images were recorded with Carl Zeiss EVO MA15. The fourier transform infrared spectra were recorded at room temperature with 4 cm^{-1} spectral resolution between 400 and 4000 cm^{-1} by a BRUKER FTIR spectrometer. Solid state ^{31}P NMR spectra were obtained at 400 MHz using a JOEL ECX400 DELTA2 NMR spectrometer with a 4 mm probe. The acquisition time was 18 ms and pulse width was 2.9 μs. The ^{31}P NMR spectra were collected in 128 scans, 5 s relaxation delays.

III. RESULTS AND DISCUSSION

3.1. X-ray diffraction, SEM analysis

Figure 1 shows the X-ray diffraction spectra of prepared glass samples. The observed broad and diffuse peaks in the diffraction pattern confirm the amorphous nature of the present glass matrices. Figure 2 shows SEM image of Li glass matrix. The SEM images for Mg, Ca and Ba glasses were not shown, since all glass samples were found similar in nature. These images have not shown any grains which confirm the amorphous nature of prepared glasses.
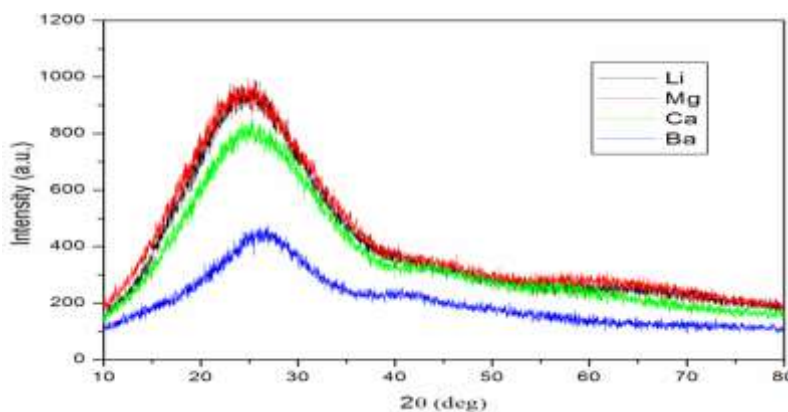

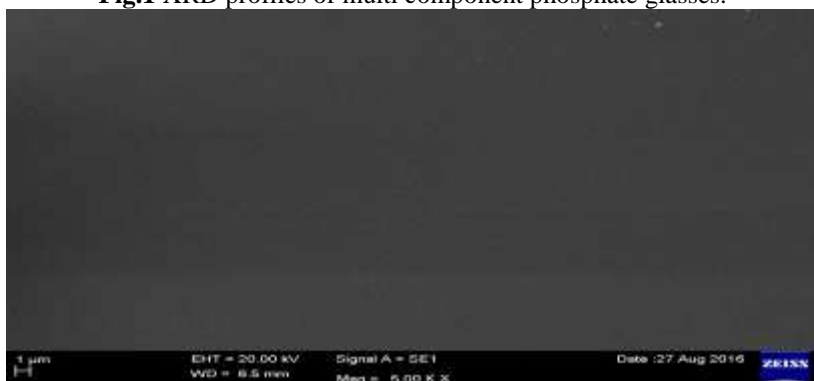**Fig.1** XRD profiles of multi component phosphate glasses.

Fig. 2 SEM Image of lithium phosphate glass.

3.2. ^{31}P NMR Spectroscopy

^{31}P solid state NMR is a precious tool in characterizing structures of phosphate-type glasses due to the chemical shifts being sensitive to the phosphorus environment. The phosphate bonding is described via Q^n species, where the superscript *n* refers to the number of bridging oxygens per tetrahedron. The solid state ^{31}P NMR spectra obtained for the different prepared glass matrices are shown in Figure. 3. It is noticed from Fig. 3 that, Li, Mg, Ca and Ba phosphate glasses have exhibited the signals with chemical shifts -20.8, -24.7, -21.8, and -22.1ppm respectively. Herein, the peaks observed from the prepared phosphate glass matrices were due to essentially of the Q^2 (metaphosphate) species [19]. The signal had single symmetric Q^2 peak which indicated the existence of no other Q^0 (phosphate tetrahedral with zero bridging oxygens), Q^1 (phosphate tetrahedral with one bridging oxygens) and Q^3 (phosphate tetrahedral with three bridging oxygens) structural units.
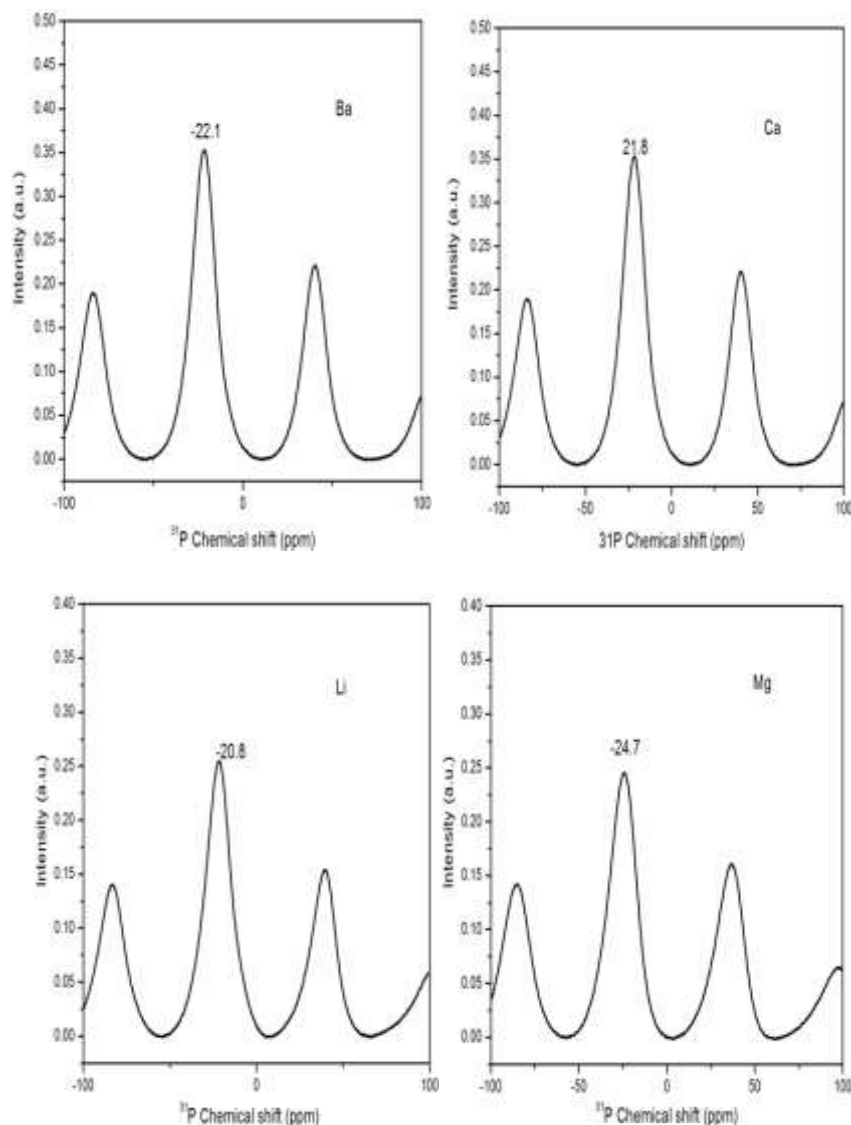

Fig. 3 NMR Spectra of multi component phosphate glasses.

3.3. Absorption spectra and Judd-Ofelt (J-O) parameters

Figures. 4a&4b show the absorption spectra of Pr^{3+} doped multi component phosphate glasses measured in the range 400-700 nm and 1200-1800 nm for visible and NIR regions, respectively. It was noticed that absorption spectra had six absorption bands peaked at ~444, ~468, ~480, ~590, ~1430 and ~1530 nm corresponding to the transitions from the ground state $^3H_4$ to the excited states $^3P_2$, $^3P_1+^1I_6$, $^3P_0$, $^1D_2$, $^3F_4$ and $^3F_3$, respectively. The absorption band, $^3P_2$ centered at nearly 22,675 cm^{-1} was the most intense in the visible region whereas in the NIR region the intense band $^3F_3$ arises at energy nearly 6,535 cm^{-1}. Observed band positions and their assignments of different absorption transitions of multi component phosphate glasses are presented in Table 1. It

was observed that the band positions and their corresponding bandwidths did not vary much with the component in the glass matrix indicating that the dopant ions were homogenously distributed in host glass matrix.
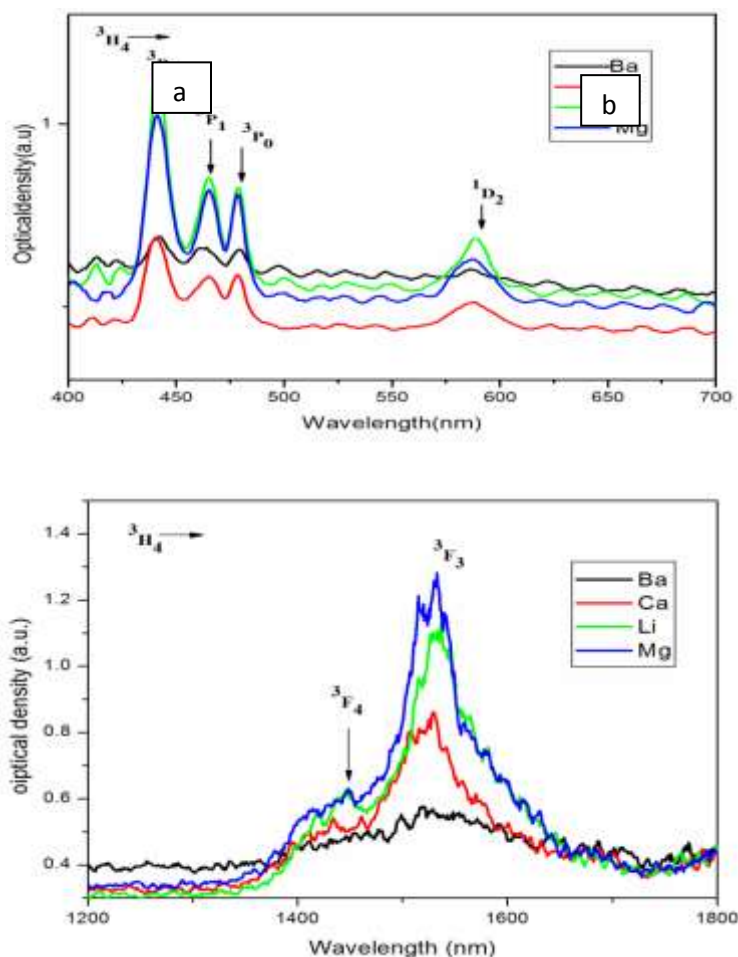

Fig. 4(a) Uv-Visible (b) NIR absorption spectra of Pr^{3+} doped multi component phosphate glasses

The experimental spectral intensities (f_{exp}) of different absorption bands of Pr^{3+} doped multi component phosphate glasses were obtained using the formula given in Ref [20]. The calculated spectral intensities (f_{cal}) were obtained using the formula given in Ref [21]. Both f_{exp} and f_{cal} values of different absorption bands Pr^{3+} doped multi component phosphate glasses are presented in Table 2. Some of the spectral intensities have sensitive character to the small change in the surrounding environment. These transitions could be called as 'hypersensitive transitions'. These transitions obey the selection rules, $\Delta J \leq 2$, $\Delta L \leq 2$ and $\Delta S = 0$, which are the same as those of a pure quadrupole transition [22]. The transition, $^3H_4 \rightarrow ^3P_2$ was the hypersensitive transition for the Pr^{3+} ion, and the transition intensity

changed significantly with the glass composition. The accuracy of fit between f_{exp} and f_{cal} values was given by root mean square (rms) deviations. From Table 2 it was observed that, among all multicomponent Pr^{3+} doped glasses, **Mg** glass showed higher spectral intensity and **Ca** glass showed lower spectral intensity for the hypersensitive transition. All transitions f_{exp} values were in good agreement with the f_{cal} values which indicated the validity of Judd-Ofelt (J-O) theory. Here the hypersensitive transition $^3H_4 \rightarrow ^3P_2$ was not considered in rms deviations calculations. The J–O parameters were obtained for all Pr^{3+} doped glass matrices from the least square approach and the results were summarized in Table 3 along with other hosts. The Ω_2 parameter strongly depends on short range effects, such as covalency of the RE ion and sensitive to the symmetry of RE ion site, while Ω_4 and Ω_6 are long-range parameters related to the bulk properties of the glass such as rigidity and viscosity [4]. Covalency was found decreasing in the

Table 1. Observed band positions (cm^{-1}) and their assignments of different excited levels of Pr^{3+} doped multicomponent phosphate glasses

S. No	Transition $^3H_4 \rightarrow$	Li	Mg	Ca	Ba
1	$^3P_2$	22675.7	22675.7	22675.7	22675.7
2	$^3P_1 + I_6$	21459.2	21505.4	21505.4	21598.3
3	$^3P_0$	20876.8	20920.5	20920.5	20833.3
4	$^1D_2$	17006.8	17064.8	17006.8	17035.8
6	$^3F_3$	6514.7	6531.7	6535.9	6544.5

order Li → Ca →Mg →Ba in Pr^{3+} doped multi component glasses. The obtained value of Ω_2 parameter in **Li** glass is 12.96x10^{-20} cm^2 and in Ba glass, it is 3.30x10^{-20} cm^2 indicating higher and lower values among the four glass matrices which indicated higher and lower covalancies of Pr-O bond. Ω_2 is found higher in the present work than that in phosphate [23], ZBLAN [24], fluoride [25], and FP glasses [26], indicating the higher asymmetry/higher covalency and lower covalency, compared with chalcogenide [27] and fluorotellurite [28] glasses, respectively. Among the four glass matrices, Ba glass matrix showed higher Ω_6 parameter indicating higher rigidity of the glass matrix.

Table 2. Experimental (f$_{exp}$) and calculated (f$_{cal}$) spectral intensities (x10^{-6}) of different absorption bands of Pr^{3+} doped multicomponent phosphate glass matrices.

Transition $^3H_4 \rightarrow$	Li		Mg		Ca		Ba	
	f$_{exp}$	f$_{cal}$	f$_{exp}$	f$_{cal}$	f$_{exp}$	f$_{cal}$	f$_{exp}$	f$_{cal}$
$^3P_2$	9.4.	5.46	11.72	5.54	5.03	3.74	9.90	7.46
$^3P_1 + I_6$	5.24	5.96	5.09	6.49	2.83	3.19	5.76	5.32
$^3P_0$	3.33	3.89	3.56	4.23	1.78	1.84	3.47	3.06
$^1D_2$	1.91	1.64	1.67	1.60	1.14	1.15	0.56	2.22
$^3F_3$	4.78	5.41	4.48	5.49	3.76	3.95	7.35	7.71
δrms	9.54	9.30	10.06	9.72	6.60	6.50	12.44	12.20

3.4. Radiative parameters

Using J-O intensity parameters, electric dipole line strengths (S_{ed}), radiative transition probabilities (A_R), radiative lifetimes (τ_R), radiative branching ratios (β_R) and absorption cross-sections ($\sum$) of certain excited states of Pr^{3+} doped all the glass matrices were obtained using the formulae given in Ref. [25]. For Li glass matrix. Branching ratios (β) and integrated absorption cross-section ($\sum$) of certain transitions which are having higher in magnitudes are reported in Table 4 for the four glass matrices. From the table it is observed that the branching ratios and absorption cross-sections of the transitions, $^3P_1 \rightarrow {}^3F_3$, $^3P_0 \rightarrow {}^3F_2$ and $^1D_2 \rightarrow {}^3F_4$ are higher in Li phosphate glass matrix. These values were found higher for $^1D_2 \rightarrow {}^3F_4$ transition in Ba glass matrix and for $^3P_0 \rightarrow {}^3F_2$ transition, these values were higher in Mg glass matrix. Total radiative transition probabilities (A_T) and radiative lifetimes (τ_R) of the excited states: $^3P_1$, $^3P_0$, $^1D_2$ and $^3F_3$ of Pr^{3+} ion were calculated in the four glass matrices and were presented in Table 5. The observations revealed that, total radiative transition probabilities were found decreasing in the order $^3P_1 > {}^3P_0 > {}^1D_2 > {}^3F_3$ for all glass matrices except for Ca glass matrix. Among all the excited states, $^3P_1$ shows higher transition probability i.e., 57129 s^{-1} in **Li** glass matrix. Higher emission probability caused the faster decay of that emission level and hence reduction of the lifetime (τ_R). Among all the excited states, $^3F_3$ state had higher radiative lifetimes. Among various transitions, the transitions $^3P_1 \rightarrow {}^3F_3$, $^3P_0 \rightarrow {}^3F_2$, $^1D_2 \rightarrow {}^3F_4$, and $^3F_3 \rightarrow {}^3H_4$, have higher magnitude of integrated absorption cross sections and also predicted branching ratios (from J–O theory) in all multicomponent Pr^{3+} doped glasses. Among different multi component glasses, Li glass matrix has higher $\sum$ values for the transition $^3P_1 \rightarrow {}^3F_3$ i.e., 53.71x10^{-16} cm^{-1}. For the remaining glass matrices, i.e., Mg, Ca, and Ba glasses, $\sum$ values are 23.671x10^{-16} cm^{-1}, 26.471x10^{-16} cm^{-1} and 19.87x10^{-16} cm^{-1}, respectively, for the transition $^3P_1 \rightarrow {}^3F_3$.

Table 3 Judd-Ofelt intensity parameters (Ω_λ, $x10^{-20}$ cm^2) of Pr^{3+} doped multicomponents phosphate glass matrices

Glass	Ω_2	Ω_4	Ω_6	Trend	Ref
Li	12.96	7.01	9.46	$\Omega_2 > \Omega_6 > \Omega_4$	present work
Mg	4.18	7.639	9.74	$\Omega_6 > \Omega_4 > \Omega_2$	present work
Ca	6.38	3.29	6.96	$\Omega_6 > \Omega_2 > \Omega_4$	present work
Be	3.30	5.40	13.90	$\Omega_6 > \Omega_4 > \Omega_2$	present work
Phosphate	3.42	4.09	4.35	$\Omega_6 > \Omega_4 > \Omega_2$	[23]
ZBLAN	2.44	4.41	5.52	$\Omega_6 > \Omega_4 > \Omega_2$	[24]
Fluoride	2.50	5.40	6.00	$\Omega_6 > \Omega_4 > \Omega_2$	[25]
Fluor-phosphate	2.75	3.21	3.36	$\Omega_6 > \Omega_4 > \Omega_2$	[26]
Halogen	9.11	7.50	5.66	$\Omega_2 > \Omega_4 > \Omega_6$	[27]
Fluorotellurite	4.76	3.00	5.50	$\Omega_6 > \Omega_2 > \Omega_4$	[28]

3.5. Emission spectra analysis

The emission spectra of Pr^{3+} doped different phosphate glasses were measured using excitation wavelength, 445 nm in the region 500-750 nm and are shown in Figure. 5. From figure 5 it is observed that, the emission spectra consist six bands corresponding to the transitions, $^3P_1 \rightarrow ^3H_5$, ($^3P_0 \rightarrow ^3H_6$) + ($^1D_2 \rightarrow ^3H_4$), $^3P_0 \rightarrow ^3F_2$, $^3P_1 \rightarrow ^3F_3$, $^3P_0 \rightarrow ^3F_3$ and $^3P_0 \rightarrow ^3F_4$ appeared at nearly 523, 608, 638, 681, 701 and 722 nm, respectively. Figure 5 revealed that the intense de-excitations have occurred mainly from $^3P_0$ excited band. The emission band in the orange-red region was due to $^3P_0 \rightarrow ^3H_6 + ^1D_2 \rightarrow ^3H_4$ and $^3P_0 \rightarrow ^3F_2$ transitions which show higher intensity when compared with other emission transitions. The intensity of the transition, $^3P_0 \rightarrow ^3F_2$ decreasing in the order Li>Ca>Mg>Ba in these phosphate glass matrices.
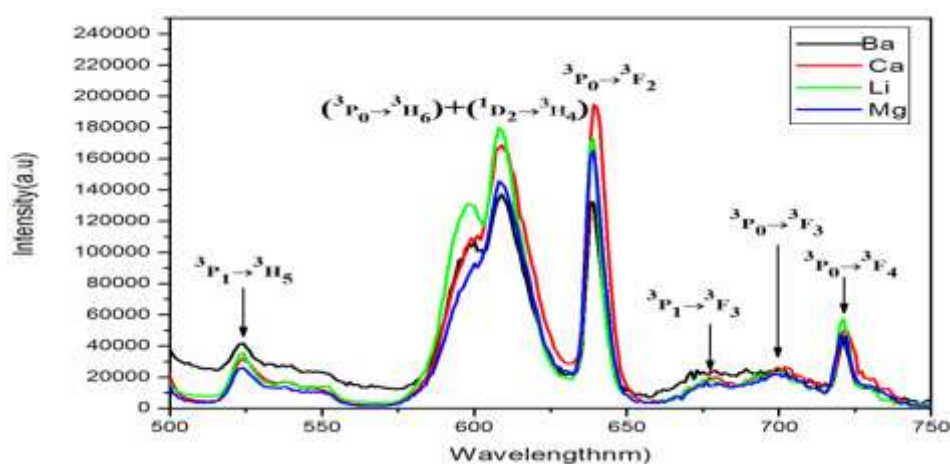
Fig. 5 Visible emission spectra of Pr^{3+} doped multi component phosphate glasses.

Luminescence parameters for the emission transitions were calculated for all the glass matrices and were shown in Table 4. It is noted that the transition, $^3P_0 \rightarrow ^3F_2$ of Pr^{3+} was the most probable emission transition than the transition $^3P_0 \rightarrow ^3H_6 + ^1D_2 \rightarrow ^3H_4$. Also, it was noted that the predicted radiative transition probability for the transition $^3P_0 \rightarrow ^3F_2$ of Pr^{3+} doped Li glass (which had high emission intensity) was 9425 s^{-1}, which was higher than another kinds of fluorotellurite glass (4576 s^{-1}) [29], borate glass (1318 s^{-1}) [30] and lower than phosphate (30380 s^{-1}) [31] and tellurite (56348 s^{-1}) glasses [32]. Higher spontaneous emission probability provides better opportunity to obtain laser action. The fluorescence branching ratio is a significant factor to any optical material, because it characterizes the possibility of attaining fluorescence from any specific transitions. Among different transitions, branching ratio of $^3P_0 \rightarrow ^3F_2$ emission transition was found highest one and could be considered as good fluorescent transition. Further, the magnitude of β_R parameter was higher for the Li glass matrix (46 %) and lower (20 %) for Mg glass matrix. Hence, Li glass could be considered as more appropriate for lasing material. The stimulated emission cross section (σ_p) of emission transition is one of the important parameters used to identify a good optical material. A good optical material has a large emission cross section. In the present work, it was observed that the transition, $^3P_0 \rightarrow ^3H_6 + ^1D_2 \rightarrow ^3H_4$, showed higher peak emission cross

section, i.e., 9.72×10^{-20} cm^2 at $\lambda_p = 523$ nm in Li glass among the four glass matrices. It was higher value when compared with other glass matrices like borate (1.24×10^{-20} cm^2) [30] and phosphate (5.54×10^{-20} cm^2) [31] glasses.

Table 4 Peak positions (λ_P, nm), effective bandwidths ($\Delta\nu_{eff}$, cm^{-1}), peak stimulated emission cross-sections (σ_P, x 10^{-20} cm^2) and branching ratios (β) of certain emission transitions of Pr^{3+} doped multicomponent phosphate glasses

Transition	Parameters	Li	Mg	Ca	Ba
3P1→3H5	λP	482	487	483	483
	$\Delta\nu eff$	349	518.8	454.6	529.1
	βR	0.2385	0.187	0.221	0.223
	σP	2.99	2.24	1.10	1.55
3P0→3H6+	λP	523	523	524	523
1D2→3H4	$\Delta\nu eff$	237.6	275.7	275.9	1507.4
	βR	0.044	0.046	0.043	0.326
	σP	9.72	8.98	4.68	1.84
3P0→3F2	λP	608	608	608	608
	$\Delta\nu eff$	410.1	316.9	431.4	361.3
	βR	0.586	0.533	0.529	0.355
	σP	1.20	1.56	1.11	1.78
3P1→3F3	λP	638	638	639	638
	$\Delta\nu eff$	59.8	94.8	92.3	65.2
	βR	0.090	0.168	0.146	0.069
	σP	8.730	5.680	5.610	0.119
3P0→3F4	λP	720	720	721	720
	$\Delta\nu eff$	67	196.5	121.2	58.1
	βR	0.041	0.065	0.061	0.027
	σP	4.64	5.130	1.29	0.14

3.6. Decay curve analysis

Fluorescence decay profiles of $^3P_0$ level of Pr^{3+}-doped different multi component glasses were recorded (λ_{ex}: 445 and λ_{em}: 681 nm) and are shown in Figure. 6. All the curves were fitted to bi-exponential function due to the hydrophilicity content of OH groups in phosphate glasses and were found to be higher than in silicate, borate, and tellurite glasses. The coordination of water molecules produce the severe vibration of the hydroxyl group, resulting in the large non-radiative transition and decreasing luminescence efficiency. In the present work, the average lifetime decay constants for $^3P_0$ excited state were found to be 18, 17, 18, and 16 µs for Pr^{3+} doped Li, Mg, Ca and Ba phosphate glasses, respectively. It is observed from present work, there is no much variation in the lifetimes of the $^3P_0$ excited state of prepared glass matrices. The lifetimes were found to be in the range 16–18 µs and reasonably in agreement with other reported lead borate glass [33] and shorter than that of lead telluroborate [34] and borate [30] glasses.
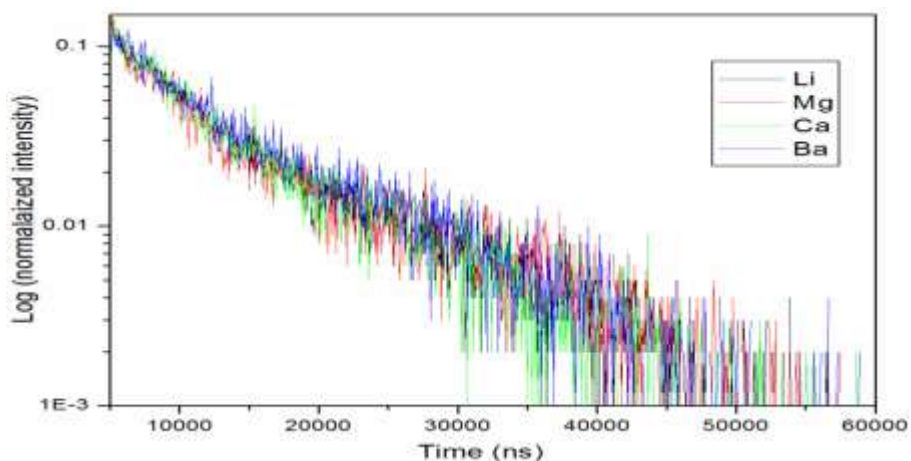
Fig. 6 Decay profile of $^1D_2$ level of Pr^{3+} doped multi component phosphate glasses.

IV. CONCLUSIONS

Pr^{3+}-doped different multi component glasses were found to be homogeneous and amorphous in nature, as confirmed by X-ray diffraction patterns and SEM. FTIR spectrum of the studied multi component glasses contain typical phosphate bonds. Phosphate acted as a network former. On the basis of ^{31}P MAS NMR analysis, a decrease in the proportion of Q^2 units in the sequence Li→Ca→Ba→Mg in these multi component host glasses was observed which indicates that these oxides were incorporated into glass as network modifier oxides. Among the three J–O intensity parameters in all the multi component glasses, the magnitude of Ω_2 parameter was higher in Li glass which could be attributed to higher covalency and asymmetry in this glass matrix. Among various excited states, radiative transition probability was decreasing in the order of $^3P_1>^3P_0>^1D_2>^3F_3$ in all multi component glasses. We conclude from above several spectroscopic characterizations that Li glass has considered as an appropriate candidate for the luminescent intensity. This observation agrees with the results from higher luminescence intensities, higher radiative transition probabilities, higher emission cross sections, and more branching ratios. Hence the present Pr^{3+} ion doped glasses can be exploited in optical devices, fluorescent display devices, optical detectors, bulk lasers, fiber amplifiers and waveguide lasers.

ACKNOWLEGEMENT

REFERENCES

[1].   Z Wang, H Guo, X Xiao, Y Xu, X Cui, M Lu, B Peng, A Yang, Z Yang, S Gu, J. Alloys Compd. 692, 1010, 2017.
[2].   K Jha, M Jayasimhadri, J. Am. Ceram. Soc. 1, 2017.
[3].   Ch B Annapurna, Sk Mahamuda, M Venkateswarlu, K Swapna, A S Rao, G Vijaya Prakash, Opt. Mater. 62, 569, 2016.
[4].   Sk Mahamuda, K Swapna, A S Rao, T Sasikala, L R Moorthy, Physica B, 428, 36, 2013.
[5].   R M Wood, Opt. Lasers Eng. 33, 383, 2000.
[6].   H Fan, G Gao, G wang, J Hu, L Hu, Opt. Mater. 32, 672, 2010.
[7].   H Lin, S Tanabe, L Lin, D L Yang, K Liu, W H Wong, Phys. Lett. Srct. A Gen. At6. Solid State Phys. 358, 474 2006.
[8].   J Pisarska, J. Phys. Condens. Matter. 21, 285101, 2009.
[9].   S Krause, C Pfau, M Dyrba, P T Miclea, S Schweizer, J. Lumin. 151, 29, 2014.
[10].   M A Marzouk, F H Elbatal, W H Eisa, N A Ghomeim, J. Non Cryst. Silides. 387, 155, 2014.
[11].   Y W Lee, M J F Digonnet, S Sinha, K E Urbanek, R L Byer and S Jiang IEEE J. Sel. Top. Quantum Electron. 15(1), 93, 2009.
[12].   B Shanmugavelu, V Venkatramu and V V Ravi Kanth Kumar Spec. Act. Part A: Mol. Bio. Spec. 122, 422, 2014.
[13].   H Lin, S Jiang, J Wu and F Song J. Phys. D. Appl. Phys. 36, 812, 2003.
[14].   A Mori, T Sakamoto, K Kobayashi, K Shikano, K Oikawa, K Hoshino, T Kanamori, Y Ohishi and M Shimizu J. Lightwave. Technol. 20(5), 794, 2002.
[15].   N Deopa, A S Rao, Sk Mahamuda, M Gupta, M jayasimhadri, D Haranath, G Vijaya Prakash. J. Alloys. Comp. 17, 307892, 2017.
[16].   X Han, L Shen, E Y B Pun, T Ma, h, Lin, Opti. Materi.36, 1203, 2014.
[17].   A Herrera, C Jacinto, A R Becerra, P L Franzen, M N Balzaretti, J. Lumin. 16,, 30437, 2016.
[18].   S kaewjaeng, S Insiripong, H J Kim, U Maghanemi, S Kothan, S Ruengsri, J Kaewkhao, Key. Engg. Materi, 675, 359, 2015.
[19].   R.K. Brow, D.R. Tallant, S.T. Meyers, and C.C. Phifer, *J. Non-Cryst. Solids* 191 (1995) 45-55.
[20].   Judd BR, Phys Rev 127, 750, 1962
[21].   Ofelt GS, J Chem Phys 37, 511, 1962.
[22].   Srinivasa Rao L, Reddy MS, Reddy MVR, Veeraiah N, Physica B 403, 2542, 2008.
[23].   Zhang F, Bi Z, Huang A, Xiao Z, J Lumin 160, 85, 2015
[24].   Anjaiah J, Laxmikanth C, Veeraiah N, Kistaiah P. J Lumin 61, 147, 2015.
[25].   Metha V, Aka G, Dawar AL, Mansingh A Opt Mater (1999) 12:53–63.
[26].   Quimby RS, Miniscalco WJ J Appl Phys (1994) 75:613.
[27].   Seeber W, Downing EA, Hesselink L, Fejer MM, Ehrt D J Non-Cryst Solids (1995) 189:218–226.
[28].   Henry ND, Adam JL, Jacquier B, Linares C Opt Mater (1996) 5:197–207.
[29].   Sourkova P, Frumarova B, Fruma M, Nemec P, Kincl M, Nazabal V, Moizan V, Doualan JL, Moncorge R J Lumin (2009) 129:1148–1153.
[30].   Mitra S, Jana S J Phys Chem Solids (2015) 85:245–253.
[31].   Man SQ, Pun EYB, Chung PS Opt Commun (1999) 168:369–373.
[32].   Jamalaiah BC, Suresh Kumar J, Babu AM, Rama Moorthy L, Jang K, Lee HS, Jayasimhadri M, Jeong JH, Choi H J Lumin (2009) 129:1023–1028.
[33].   Dzika GD, Romanowski WR, Pisarska J, Pisarski WA . J Lumin (2007) 122–123:62–65
[34].   Vijaya Kumar MV, Rama Gopal K, Reddy RR, Reddy GVL, Hussain NS, Jamalaiah BC, J. Non-Cryst Solids (2013) 364:20–27.